PHYSICAL REVIEW B **80**, 241203(R) (2009)

Observation of the magnetic soft mode in (Cd,Mn)Te quantum wells using spin-flip Raman scattering

C. Kehl,[1] G. V. Astakhov,[1] K. V. Kavokin,[2] Yu. G. Kusrayev,[2] W. Ossau,[1] G. Karczewski,[3] T. Wojtowicz,[3] and J. Geurts[1]
[1]*Physikalisches Institut (EP3), Universität Würzburg, 97074 Würzburg, Germany*
[2]*A.F. Ioffe Physico-Technical Institute, Russian Academy of Sciences, 194021 St. Petersburg, Russia*
[3]*Institute of Physics, Polish Academy of Sciences, 02668 Warsaw, Poland*
(Received 30 November 2009; published 29 December 2009)

We report the experimental observation of a magnetic soft mode of collective spin excitations in (Cd,Mn)Te quantum wells, containing a 2D hole gas interacting with magnetic ions. We found that with increasing hole concentration the eigenfrequency of the paramagnetic spin resonance decreases, which is predicted to occur prior to the ferromagnetic phase transition. Such a magnetic soft mode is detected in spin-flip Raman-scattering experiments as a reduction in the Mn g factor. The results are described in terms of collective dynamics of strongly coupled spin systems with positive feedback. Based on this approach the evolution of such excitations with hole concentration is calculated.

DOI: 10.1103/PhysRevB.80.241203 PACS number(s): 75.50.Pp, 75.70.Cn, 78.30.Fs

It is well established that ferromagnetic order of localized magnetic moments can be mediated by free carriers through indirect exchange coupling, known as Ruderman-Kittel-Kasuya-Yosida (RKKY) interaction. This mechanism is considered to be responsible for the ferromagnetism of diluted magnetic semiconductors (DMSs), such as (Ga,Mn)As and (In,Mn)As,[1] (Pb,Sn,Mn)Te,[2] (Zn,Mn)Te,[3] and (Cd,Mn)Te.[4] The Curie temperatures in DMS ferromagnets based on II-VI semiconductors are rather low, $T_C \sim 1$ K. While for practical application T_C should be above 300 K, II-VI DMSs are attractive objects to study the RKKY interaction because of their bright magneto-optical characteristics and the possibility of varying in a wide range the carriers concentration independent of the concentration of magnetic impurities. Indeed, DMS magnetic properties in the paramagnetic[5–9] and ferromagnetic[4,10] states have been investigated in great detail. However, the question of how spin excitations evolve between these two phases was not addressed experimentally so far.

A general property of phase transitions is a softening of the corresponding oscillation mode. It has been shown theoretically that the exchange interaction between magnetic ions and a two-dimensional hole gas (2DHG) results in a drastic decrease in the Larmor precession (i. e., softening of the magnetic mode) in the vicinity of the ferromagnetic phase transition.[11] By lowering the temperature or by increasing the hole concentration the spin-resonance frequency ω of Mn ions decreases to zero according to

$$\omega = \Omega\sqrt{1-\xi}. \tag{1}$$

Here, Ω is the unperturbed resonance frequency corresponding to the Mn spin precession with the g factor $g_{\mathrm{Mn}}^{(0)} \approx 2$ and ξ is a parameter depending on the exchange integral and the paramagnetic spin susceptibilities of Mn ions and 2DHG. Hence, the crucial parameters allowing control of magnetic softening are the temperature of the spin system and the 2DHG density. A temperature-dependent spin resonance was observed by time-resolved Kerr rotation in p-type (Cd,Mn)Te QWs.[12] However, the high-temperature (paramagnetic) spin-resonance frequency from these experiments does not agree with the "free" Mn precession frequency ($g_{\mathrm{Mn}}^{(0)} \approx 2$), which is difficult to explain by the magnetic mode softening. In our studies we use the alternative approach, applying constant temperatures while we tune the hole concentration by varying the additional illumination power.

In this Rapid Communication, we report the observation of the magnetic soft mode in (Cd,Mn)Te quantum wells (QWs) with a 2DHG. It reveals itself in spin-flip Raman-scattering (SFRS) experiments as a decrease in the Mn g factor beyond 5% with increasing 2DHG concentration of up to 10^{11} cm^{-2}. The effect disappears with rising temperature and provides a sensitive probe for spin excitation dynamics and paramagnetic susceptibility in the vicinity of the ferromagnetic phase transition.

Single 120 Å $Cd_{0.993}Mn_{0.007}Te$ QWs were grown by molecular-beam epitaxy (MBE) on (001)-oriented GaAs substrates with thick CdTe buffers and $Cd_{0.8}Mg_{0.2}Te$ barriers. The QWs were covered by thin $Cd_{0.8}Mg_{0.2}Te$ cap layers. Though these QWs are not specially doped, owing to the surface states they contain a 2DHG.[13] To present our results we choose a QW with a cap layer thickness of 175 Å, where the surface-state induced p-type doping is most effective.

Photoluminescence (PL) and Raman spectra were excited by a tunable dye laser pumped by an Ar-ion laser and detected by a charge-coupled device linked to a subtractive triple spectrometer, providing a spectral resolution of about 0.5 cm^{-1} (65 μeV). The excitation and detection were linearly cross-polarized. We performed experiments in the two-color mode; i.e., an additional above-barrier illumination by means of light split off from the Ar-ion laser (2.41 eV) was utilized to tune the hole concentration in the QW. We used the same optical path to focus the dye laser and Ar-ion laser beams onto overlapped spots. External magnetic fields of up to 4.5 T applied in the sample plane $B \| x$ (Voigt geometry) were provided by a split coil magnet. The experiments were performed in the temperature range between $T=1.7$ K and 4.2 K.

A PL spectrum for below-barrier excitation ($\hbar\omega_b = 1.6222$ eV) in the low power limit ($P_b = 0.5$ μW)

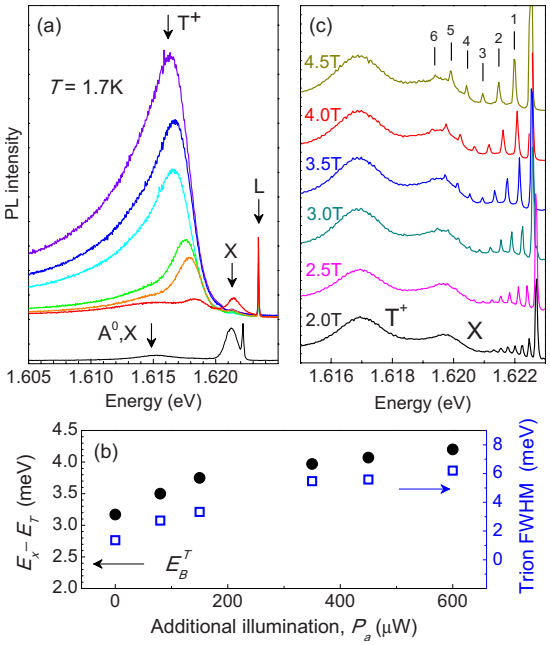

FIG. 1. (Color online) (a) PL spectra at $B=0$ for increasing excitation power P_a of the above-barrier excitation (upper curves). Lower curve: PL spectrum for below-barrier excitation $P_b=0.5$ μW without additional illumination. The spectrum is multiplied by a constant and vertically shifted for clarity. (b) Spectral separation between the exciton and trion lines (left axis) and the full width at half maximum (FWHM) of the trion line (right axis) as function of $P_a(P_b=10$ μW).(c) Raman spectra for various B fields in the QW plane (Voigt geometry). Six Mn^{2+} paramagnetic resonance (PR) lines are marked for $B=4.5$ T. Excitation conditions correspond to $n_h=5.0\times10^{10}$ cm^{-2}.

contains the neutral exciton (X) and the acceptor-bound exciton (A^0,X) lines [lower curve in Fig. 1(a)]. With increasing illumination power an additional line labeled as T^+ appears [upper curves in Fig. 1(a)]. The T^+ line represents the positively charged trion which is the fingerprint of the presence of a 2DHG in the QW; the stronger T^+ line the higher the concentration is.[16,17] In further experiments we fixed the below-barrier excitation $P_b=10$ μW to keep the excitation conditions unchanged, while the hole concentration is tuned by an additional above-barrier illumination P_a. With increasing P_a the T^+ line grows at the expense of the X line intensity, and for sufficient P_a the exciton line vanishes. Further evidence of the presence of a 2DHG in the QW is the increase in the trion line width. As shown in Fig. 1(b), the FWHM of the T^+ line as function of P_a increases from 1.4 meV at $P_a=0$ μW to 6 meV at $P_a=600$ μW. This is ascribed to the efficient scattering by resident carriers in the QW.[14,15]

The mechanism of optical tuning of the carrier density in QW heterostructures results from spatial separation of photogenerated electrons and holes.[18,19] When a nominally undoped QW is located close to the surface (as in our case), the photogenerated electrons can tunnel through the barrier to surface states, increasing the number of holes residing in the QW. This surface p-type doping extremely depends on the cap layer thickness and excitation conditions.[13]

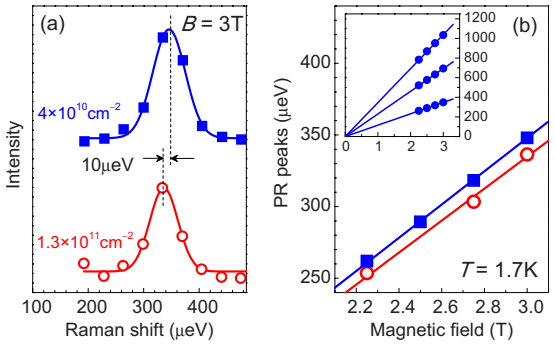

FIG. 2. (Color online) (a) The first PR line in Raman spectrum for $n_h=4\times10^{10}$ cm^{-2} (upper curve) and for $n_h=1.3\times10^{11}$ cm^{-2} (lower curve). $B=3$ T. (b) Raman shift of the first PR line vs magnetic field for two different hole concentrations as in panel (a). Inset: overview of the three PR lines for $n_h=4\times10^{10}$ cm^{-2}.

The spectral separation between the exciton and trion lines depends on the carrier concentration as[19,20]

$$E_X - E_T = E_B^T + \varepsilon_F. \tag{2}$$

Here, E_B^T is the "bare" trion binding energy and ε_F is the Fermi energy. Figure 1(b) shows the exciton-trion separation as a function of the above-barrier excitation power P_a. From the spectrum in the low power limit ($P_b=0.5$ μW and $P_a=0$ μW) we obtain $E_B^T=2.4$ meV. This allows us to determine the "nonequilibrium" Fermi energy $\varepsilon_F=\pi\hbar^2 n_h/m_h$ of the 2DHG according to Eq. (2) and with known in-plane effective hole mass $m_h=0.2m_0$ (Ref. 21) to obtain the hole density n_h as a function of illumination power. In particular, for $P_b=10$ μW and without above-barrier illumination we find $E_X-E_T=3.1$ meV, which yields $n_h=4\times10^{10}$ cm^{-2}. With the strongest additional illumination $P_a=600$ μW (P_b remains constant) we find $n_h=1.5\times10^{11}$ cm^{-2}. The two-color experiment is required to study the collective Mn spin excitations as function of 2DHG density: a dye laser of constant intensity P_b is used for the resonant spin-flip Raman excitation, and the hole density is tuned continuously by the additional illumination P_a.

First, we describe the Raman spectra without additional illumination [Fig. 1(c)]. In external B fields applied in the Voigt geometry up to $n=6$ equidistant Raman lines occur, shifting linearly with increasing field. This multiple PR process originates from the strong exchange interaction between the heavy-hole (hh) exciton and Mn ions.[6] In the QW this interaction is strongly anisotropic: in the extreme case the hh spin components in the QW plane (x-y plane) vanish ($J_x=J_y=0$). Hence, in an external field $B\|x$, the exciton with $J_z\neq0$ induces transitions among states with different projections of the Mn spin on the field direction, resulting in PR Raman lines.

The $n=1$ PR Raman line obtained at $B=3$ T is shown in Fig. 2(a) in the enlarged scale (solid squares). These data are obtained without additional illumination ($P_a=0$) corresponding to the hole density $n_h=4\times10^{10}$ cm^{-2}. The Gaussian fit (solid line) allows the accurate determination of the Raman shifts E_n of the PR lines. Its application to the first three PR peaks yields their linear shift with growing B field, as shown

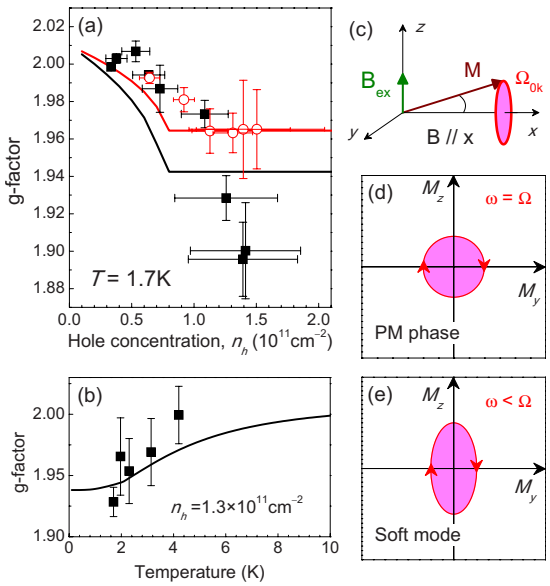

FIG. 3. (Color online) (a) Mn g factor as function of 2DHG density obtained in the B-field ranges of 2.25–3 T (solid squares) and 3–3.5 T (open circles). Solid lines: calculations for $B=2.6$ and 4 T (see text for details). $T=1.7$ K. (b) g_{Mn} as function of temperature. Solid line: calculation for $B=2.6$ T. (c) Diagram of the collective spin excitations. B_{ex} denotes the exchange field of spin-polarized holes creating an additional torque acting on the magnetic moment M of Mn ions. (d) and (e) Oscillations of M in the y-z plane in case of the paramagnetic phase and the soft mode, respectively.

in the inset of Fig. 2(b). From the linear fits according to $E_n=ng_{\mathrm{Mn}}\mu_B B$ (solid lines)[6] the Mn-g-factor is determined as $g_{\mathrm{Mn}}=1.998\pm0.001$. This value is close to $g_{\mathrm{Mn}}^{(0)}=2.010$ obtained in CdTe:Mn bulk crystals.[22]

The lower part of Fig. 2(a) shows the PR Raman line ($n=1$) with additional illumination ($P_a\neq0$) and thus for increased hole density $n_h=1.3\times10^{11}$ cm^{-2} (open circles). Its intensity is reduced by about an order of magnitude due to photomodulation of the Raman process.[23] Note that the Gaussian fit yields a 10 μeV energy downshift with respect to the upper curve. A systematic downshift of the first PR line in the presence of a dense 2DHG is clearly seen in the enlarged scale of Fig. 2(b). From the linear fit $E_1=g_{\mathrm{Mn}}\mu_B B$ we evaluate $g_{\mathrm{Mn}}=1.93\pm0.01$, which is 4% smaller than the one without additional illumination.

By varying the above-barrier illumination power P_a we measure the concentration dependence of the Mn g factor summarized in Fig. 3(a). Solid squares (open circles) correspond to g_{Mn} obtained from the linear fit in the B-field range 2.25–3 T (3–3.5 T). Obviously, the decrease in g_{Mn} is B-field dependent, high B fields lead to its suppression. The low-field value reduces down to $g_{\mathrm{Mn}}=1.89\pm0.02$ for $n_h=1.4\times10^{11}$ cm^{-2}. The change $\Delta g_{\mathrm{Mn}}\approx-0.05$ (as compared with $g_{\mathrm{Mn}}^{(0)}$) is larger and of opposite sign compared to the Knight shift of g_{Mn} (for the given concentration it is in the order of 10^{-3}).[24] Furthermore, we find that the g decrease is suppressed with increasing temperature [Fig. 3(b)].

We now present a theoretical description of the effect. Qualitatively, the frequency shift of Mn spin precession was predicted earlier.[11] It arises due to an additional torque exerted on the Mn spins by the hole spins [Fig. 3(c)]. Because of the g-factor anisotropy, the Mn spin component perpendicular to B induces a predominant polarization of hole spins along the structure axis z. The oscillating exchange field of spin-polarized holes, applied to Mn spins, makes them circumscribe elliptic rather than circular, trajectories around B, which slows down their Larmor precession [Figs. 3(d) and 3(e)].

Two main issues which are specific for SFRS experiments have to be addressed here: (i) spin oscillations are excited by localized excitons and therefore can have nonzero spatial frequencies and (ii) experiments are performed in strong B fields, and therefore the Zeeman splitting of the holes in Voigt geometry is comparable to their Fermi energy. Resident 2D holes, as well as the localized exciton that initiates SFRS, interact with a large number of Mn^{2+} ions: $4\pi^2 Lk_F^{-2}N_0 x\gg1$ and $\pi LR^2N_0x\gg1$ (where L is the QW width and R is the exciton localization radius). For this reason it is convenient to write the Hamiltonian of the spin system in terms of spin-density components S_{lk},

$$\hat{\mathcal{H}}(\{\vec{S}_{lk}\}) = -g_{\mathrm{Mn}}^{(0)}\mu_B\sum_l S_{l0}^x B - \frac{\beta}{3}\frac{g_\perp}{g_\parallel}J_x\sum_l \Psi_h^2(z_l)S_{l0}^x$$

$$-\frac{g_\perp}{2}\mu_B A J_x B + \delta E_{ex}. \tag{3}$$

The subsequent terms represent (i) the Zeeman energy of the Mn spins (S_{l0} is the spin density of the lth monolayer), (ii) the exchange interaction energy (for Mn spins along x); J_x is the x component of the hole spin density, (iii) the hh Zeeman energy (where A is the area of the structure). The exchange energy correction δE_{ex} is due to deflection of spin-density components from x [Fig. 3(c)], B is the B field along x; $g_\parallel$ and $g_\perp$ are the longitudinal and transversal hh g factors, respectively.

Since in equilibrium the mean spin direction is along x, δE_{ex} is quadratic in the y and z components of the spin density: these energy corrections arise because of the interaction of the Mn ion spins with the induced 2DHG polarization, perpendicular to x, and are proportional to the 2DHG susceptibility. We calculated χ_k, the transversal 2DHG spin susceptibility to the exchange field of magnetic ions at the spatial frequency k, using perturbation theory. At low temperature ($k_BT\ll\Delta_V$, where Δ_V is the hole spin splitting in Voigt geometry) it is given by:

$$\chi_k = \frac{m}{8\pi\hbar^2\varepsilon_k}[\varepsilon_k+\Delta_V-\sqrt{(\varepsilon_k+\Delta_V)^2-4\varepsilon_k\varepsilon_F}] \tag{4}$$

and

$$\chi_k = \frac{m}{8\pi\hbar^2\varepsilon_k}[\varepsilon_k+\Delta_V-|\varepsilon_k-\Delta_V|] \tag{5}$$

at $\varepsilon_F\leq\Delta_V$ and $\varepsilon_F\geq\Delta_V$, respectively. Here $\varepsilon_k=\frac{\hbar^2k^2}{2m}$, and $\varepsilon_F=\frac{2\pi\hbar^2}{m}n_h$ is the 2DHG Fermi energy.

Spins of different monolayers are coupled by indirect exchange via the 2DHG. The coupling strength is determined by the 2DHG spin susceptibility and by the mutual orienta-

tion of spins in different monolayers. Orthogonal linear combinations of spin densities of the monolayers form oscillatory modes corresponding to certain eigenfrequencies of the coupled spin system. As discussed in Ref. 11, the pulsed exchange field of the photoexcited hole induces oscillations of the mode, most strongly coupled with the 2DHG $\vec{\Phi}_{0\vec{k}}=\Sigma_l\Psi_l^2\vec{S}_{l\vec{k}}/\Sigma_l\Psi_l^2$. Its eigenfrequency can be obtained by solving Hamiltonian (3) for Φ_{0k}, where δE_{ex} is calculated using Eqs. (4) and (5). Then, the eigenfrequency can be presented as $\Omega_{0k}=g_{0k}^*\mu_B B/\hbar$, with the effective g factor

$$g_{0k}^* \approx g_{\mathrm{Mn}}^{(0)}\sqrt{1-\frac{\chi_k\beta^2}{\mu_B g_{\mathrm{Mn}}^{(0)}B\tilde{L}}N_0x\langle s_x\rangle}. \tag{6}$$

Here, $\langle s_x\rangle$ is the mean spin of a Mn ion, $\tilde{L}=a(\Sigma_l\Psi_l^4)^{-1}\approx\frac{2}{3}L$, where L is the QW width and a is the lattice constant. The dominating mode in SFRS is the one with $|k|\simeq 1/r_h$, where r_h is the localization radius of the photoexcited hole. As seen from Eqs. (4)–(6), Ω_{0k} decreases with n_h for $\varepsilon_F\leq\Delta_V$ (besides the slope and shape of the curve depend on k) and does not depend on n_h for $\varepsilon_F\geq\Delta_V$. We performed theoretical calculations using the experimentally obtained ratio $g_\parallel/g_\perp=10$ (which defines Δ_V). Their results with $r_h=10$ nm [shown by solid lines in Figs. 3(a) and 3(b)] describe all tendencies observed in our experiments.[25] Note that the g-factor shift is larger for lower B fields. The theory predicts that at very low B fields, inaccessible in SFRS experiments, g should turn to zero. This behavior, high-field traces of which we detect in our experiment, is a fingerprint of the transition to the ferromagnetic phase.

In conclusion, we observed the softening of the paramagnetic resonance in (Cd,Mn)Te QWs. The effect, detected as a decrease in the Mn g factor in SFRS experiments, is caused by the collective character of spin excitations in 2DHG. We calculated the dispersion of such excitations, which is in agreement with experimental data. We believe that our findings can be used as a sensitive tool to study the dynamics of spin excitations and paramagnetic susceptibility in the vicinity of the ferromagnetic phase transition.

This work was supported by the Deutsche Forschungsgemeinschaft (Grants No. 436 RUS113/958/0-1 and No. AS 310/2-1), BayEFG, and by the Russian Foundation for Basic Research.

[1] H. Ohno *et al.*, Appl. Phys. Lett. **69**, 363 (1996).
[2] T. Story, R. R. Galazka, R. B. Frankel, and P. A. Wolff, Phys. Rev. Lett. **56**, 777 (1986).
[3] D. Ferrand *et al.*, Phys. Rev. B **63**, 085201 (2001).
[4] A. Haury, A. Wasiela, A. Arnoult, J. Cibert, S. Tatarenko, T. Dietl, and Y. M. dAubigne, Phys. Rev. Lett. **79**, 511 (1997).
[5] D. R. Yakovlev, K. V. Kavokin, I. A. Merkulov, G. Mackh, W. Ossau, R. Hellmann, E. O. Gobel, A. Waag, and G. Landwehr, Phys. Rev. B **56**, 9782 (1997).
[6] J. Stühler, G. Schaack, M. Dahl, A. Waag, G. Landwehr, K. V. Kavokin, and I. A. Merkulov, Phys. Rev. Lett. **74**, 2567 (1995).
[7] A. V. Kudinov *et al.*, Phys. Solid State **45**, 1360 (2003).
[8] S. A. Crooker, D. D. Awschalom, J. J. Baumberg, F. Flack, and N. Samarth, Phys. Rev. B **56**, 7574 (1997).
[9] F. J. Teran, M. Potemski, D. K. Maude, D. Plantier, A. K. Hassan, A. Sachrajda, Z. Wilamowski, J. Jaroszynski, T. Wojtowicz, and G. Karczewski, Phys. Rev. Lett. **91**, 077201 (2003).
[10] H. Boukari, P. Kossacki, M. Bertolini, D. Ferrand, J. Cibert, S. Tatarenko, A. Wasiela, J. A. Gaj, and T. Dietl, Phys. Rev. Lett. **88**, 207204 (2002).
[11] K. V. Kavokin, Phys. Rev. B **59**, 9822 (1999).
[12] D. Scalbert, F. Teppe, M. Vladimirova, S. Tatarenko, J. Cibert, and M. Nawrocki, Phys. Rev. B **70**, 245304 (2004).
[13] S. Tatarenko *et al.*, Opto-Electron. Rev. **11**, 133 (2003).
[14] R. A. Suris *et al.*, Phys. Status Solidi B **227**, 343 (2001).
[15] W. Ossau *et al.*, Phys. B **298**, 315 (2001).
[16] K. Kheng, R. T. Cox, Y. Merle dAubigne, F. Bassani, K. Saminadayar, and S. Tatarenko, Phys. Rev. Lett. **71**, 1752 (1993).
[17] G. V. Astakhov, D. R. Yakovlev, V. P. Kochereshko, W. Ossau, J. Nurnberger, W. Faschinger, and G. Landwehr, Phys. Rev. B **60**, R8485 (1999).
[18] P. Kossacki, J. Cibert, D. Ferrand, Y. Merle dAubigne, A. Arnoult, A. Wasiela, S. Tatarenko, and J. A. Gaj, Phys. Rev. B **60**, 16018 (1999).
[19] G. V. Astakhov *et al.*, Phys. Rev. B **65**, 165335 (2002).
[20] V. Huard, R. T. Cox, K. Saminadayar, A. Arnoult, and S. Tatarenko, Phys. Rev. Lett. **84**, 187 (2000).
[21] G. Fishman, Phys. Rev. B **52**, 11132 (1995).
[22] J. Lambe and C. Kikuchi, Phys. Rev. **119**, 1256 (1960).
[23] A. V. Koudinov, Y. G. Kusrayev, D. Wolverson, L. C. Smith, J. J. Davies, G. Karczewski, and T. Wojtowicz, Phys. Rev. B **79**, 241310(R)(2009).
[24] T. Story, C. H. W. Swuste, P. J. T. Eggenkamp, H. J. M. Swagten, and W. J. M. de Jonge, Phys. Rev. Lett. **77**, 2802 (1996).
[25] A quantitative difference between experimental points and theoretical calculations in Fig. 3(a) may be related to the B-field-dependent ratio $g_\parallel/g_\perp$ due to the mixing of heavy-hole and light-hole states, which was not considered in our model. We use the ratio $g_\parallel/g_\perp=10$ found from the comparison of high-field shifts of the trion line in the Faraday and Voigt geometries.